

Low-power solar flares in the $H\alpha$ line: research results

A.V. Borovik

Institute of Solar-Terrestrial Physics SB RAS, Irkutsk
e-mail: aborovik@iszf.irk.ru

Received 3 November 2022

ABSTRACT

The paper summarizes the results of long-term studies of low-power flares in the $H\alpha$ line (optical class S) obtained using data from the international flare patrol, observational materials in the 6563 Å line of the Baikal Astrophysical Observatory of the ISTP SB RAS and GONG telescopes, observations from the SDO, SOHO, and Kitt Peak Observatory. As a result of the performed studies, the refined, statistically reliable and most complete to date data on the spatio-temporal parameters of solar flares have been obtained, and their total energy in the optical wavelength range has been estimated. Low-power flares were found to form dense clusters on the Sun, which are centers of flare activity (CFA) associated with regions of emerging magnetic fluxes. It was also found that such flares occur near the local small-scale short-lived polarity inversion lines (LPIL) of the longitudinal magnetic field. One of the identified regularities of their occurrence is the increase in the magnetic field gradient in certain sections of the LPIL in the flare region. The duration of growth is from 40 minutes to 1.5 hours. The magnetic field reaches its maximum gradient (1.3–1.5 G/km) at the time of flare occurrence.

The results of the study show that low-power flares have development scenarios similar to large flares: they are accompanied by activation and eruption of filaments, have an explosive phase, are accompanied by radiation of different power in the X-ray and radio ranges as well as by proton fluxes. Among them there are flares that cover the sunspot umbrae, two-ribbon and white-light flares. The results obtained can be used to construct physical models, diagnose nonstationary processes on the Sun, and predict solar activity and geoeffective solar events.

Key words: solar flares, magnetic fields

1 Introduction

Solar flares represent a wide ensemble of phenomena that differ significantly in area, energy, and power. One and a half percent of flares with energy $\sim 10^{32}$ erg are attributed to powerful flares (optical classes 2–4): relatively rare phenomena but often accompanied by geomagnetic disturbances of the Earth's atmosphere. Although the nature and mechanisms of powerful flares are not yet fully understood, there is a fairly complete understanding of such flares.

The most numerous and still poorly studied class of solar flares is low-power flares with energy $\sim 10^{29}$ erg (optical class S). They are usually considered as background events, and in rare cases, as phenomena accompanying large flares. The main results of the study of low-power flares in the $H\alpha$ line were obtained back in the 1980s. Since then, the topic of low-power flares in the $H\alpha$ line has practically not been addressed by anyone.

With the beginning of spacecraft flights, the attention of astrophysicists was drawn to the theory of the heating of the solar corona, and more attention began to be paid to X-ray microflares and nanoflares, which are flares with characteristic sizes of several thousand kilometers, according to the GOES classification belonging to classes B and A

and to the sensitivity limit of GOES detectors. Currently, the nature and role of microflares and nanoflares are still far from being clarified and remain a separate important research topic (Bogachev et al., 2020).

In the monograph by Smit, Smit (1966), small flares are characterized as small homogeneous bright nodes not associated with the chromospheric structure. Their light curves differ from those of larger flares in time scale and brightness. The duration of small flares ranges from six to ten minutes. The average intensity is 46% of the continuous spectrum according to the Sacramento Peak Observatory data and 56% according to the McMath-Hulbert data. A correlation between the intensity and area of flares is practically absent. Small flares, like large ones, occur near the polarity inversion lines of the longitudinal magnetic field component (Howard, Harvey, 1964). Flare nodes are not always interconnected and do not always form ribbons. At the limb, small flares appear as bright points that quickly turn into bright hills, acquiring conical and cylindrical shapes (Severnyi, Shaposhnikova, 1961; Howard, Harvey, 1964; Smit, Smit, 1966). Over time, they can show expansion, pulsations, ejections, and loops.

In the 1970s, during the flight of the Skylab orbital station (CINOF program), which coincided with a period of low solar activity, new data on small flares were obtained (Svestka,

1975). It was found that in active regions, low-power flares occur in series. Individual flares have a loop structure, and they are accompanied by soft X-ray and microwave radiation, by type III radio bursts. Flare nodes are located near the polarity inversion lines at the boundaries of neighboring supergranular cells.

According to modern concepts, low-power flares are attributed to simple loop-type structures. In soft X-rays, they are characterized by small volumes, low heights, high energy densities, and short time scales. The energy of such a flare is usually released in the impulsive phase. A single hard X-ray burst lasting about a minute is typical. Small flares, like large ones, are believed to occur in an active region during the emergence of a new magnetic flux, which, interacting with the overlying field, forms a current sheet. As a result, in the turbulent plasma of the current sheet, rapid annihilation of the magnetic field occurs, accompanied by the ejection of matter and a flux of particles into the lower part of the chromosphere, causing an optical flare there (Heyvaerts et al., 1977; Prist, 1985).

Analysis of the results obtained by different authors shows that individual low-power flares, differing from large flares in scale, by appearance in conditions of a relatively simple magnetic field configuration, by a group character of appearance, etc., reveal a number of features characteristic of large flares. These include the connection with polarity inversion lines, loop structure, enhancement of hard electromagnetic radiation, and generation of radio bursts (Altyntsev et al., 1982). This indicates that low-power flares may not fundamentally differ from large solar flares. And even in the case when certain phenomena (for example, the white-light continuum) are not observed in a weak flare, the process can proceed in a similar way. Therefore, the study of the patterns of occurrence of low-power flares at different phases of the active region development, their spatio-temporal distribution over the solar surface, geoeffective manifestations, as well as the physical nature, not only constitute an important direction of fundamental research for understanding the mechanisms of solar flares but can also provide an opportunity to use the results for predicting solar activity.

In this study, we aim to understand the development of the flare process in its relatively simple manifestation as well as to clarify the question of whether flares of different power are based on a single physical mechanism or whether these flares are different in nature.

2 Data

The paper provides a brief summary of the main results of the study of low-power flares in the $H\alpha$ line (optical class S) performed using observations from the Baikal Astrophysical Observatory of ISTP SB RAS, other ground-based and space observatories. We used data from the international flare patrol¹, the GOES series of satellites², observational materials acquired at the Baikal Astrophysical Observatory of ISTP SB RAS (BAO) and GONG telescopes³ in the $H\alpha$ line (6563 Å),

¹ http://www.wdcb.ru/stp/solar/solar_flare_events.ru.html

² <https://www.ngdc.noaa.gov/stp/space-weather/solar-data/solar-features/solar-flares/x-rays/goes/xrs/>

³ <https://gong2.nso.edu/HA/haf/>

observations with HMI and AIA instruments⁴ of the Solar Dynamics Observatory (SDO).

To study the dynamics of magnetic fields during flares, we used photospheric data (SDO/HMI – full-disk images of the Sun in the continuum), SDO/HMI magnetograms with an angular resolution of $0.5'' \cdot \text{pixel}^{-1}$ ($\sim 350 \text{ km} \cdot \text{pixel}^{-1}$), and data on magnetic fields from the Kitt Peak Observatory⁵ and SOHO/MDI⁶. To identify flares in the transition region of the solar atmosphere, SDO/AIA images in the 171 Å line were used.

3 Statistical studies

Spatio-temporal characteristics of flares carry important information about the dynamics and energetics of flare processes. Such studies were carried out back in the period of the formation of the international flare patrol (1957–1958). However, as the analysis of the results showed (Smit, Smit, 1966; Svestka, 1975; Altyntsev et al., 1982; Borovik, Zhdanov, 2017a), the data were heterogeneous, burdened with errors, and the statistics were low (several hundred, in rare cases several thousand flares). Since then, the parameters of solar flares have not been refined. Therefore, it made sense to repeat the study.

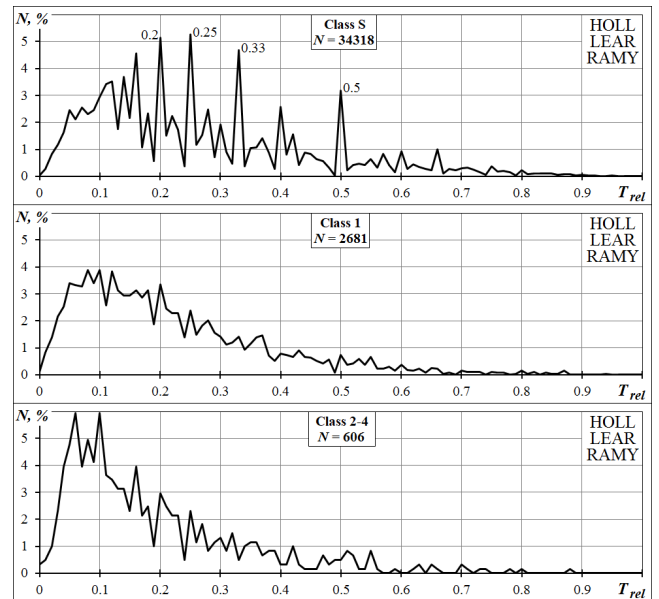


Fig. 1. Distribution of the relative rise time of solar flares of area classes S, 1, 2–4 within 65° from the central meridian according to the data from the HOLL, LEAR, and RAMY observatories; N is the number of flares.

Data from the international flare patrol for the period 1972–2010 were used (123 801 flares). Using the developed

⁴ <http://jsoc.stanford.edu>

⁵ https://www.ngdc.noaa.gov/stp/space-weather/online-publications/stp_sgd/

⁶ <http://jsoc.stanford.edu>

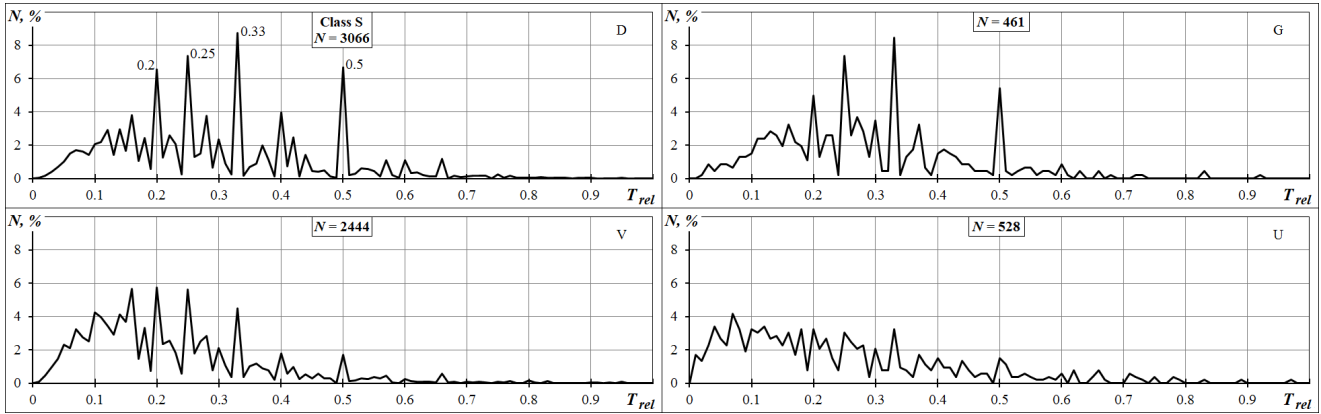


Fig. 2. Distribution of the relative rise time for four types of small flares recorded within 65° from the central meridian. D – a flare with one center of increased brightness within the flare region, G – a sunspotless flare, V – an explosive-type flare, U – a two-ribbon flare.

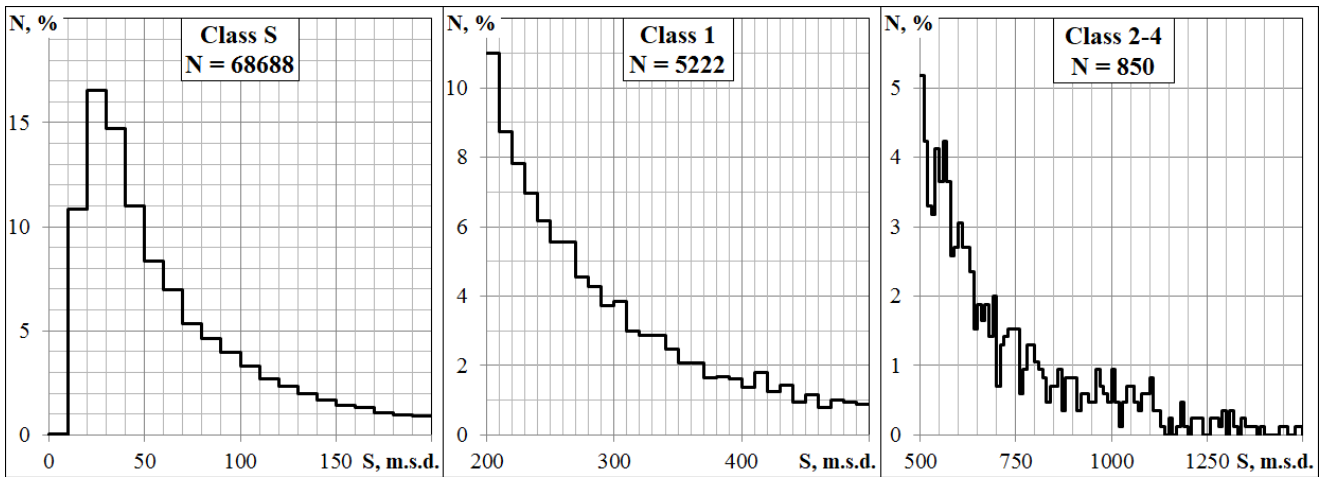


Fig. 3. Distribution of solar flares of classes S, 1, 2–4 by area, taking into account the perspective reduction within 65° from the central meridian (Borovik, Zhdanov, 2017a).

computer programs, errors in the original catalogs were corrected, duplication of events was excluded, cases when stations did not report the brightness class, area class, start time, maximum time, end time of the flare, etc., were taken into account.

As a result of the statistical study, the most complete to date and statistically reliable data on the rise time of flares to maximum, decay time, and duration were obtained (Borovik, Zhdanov, 2017a, b, 2018a, b). It was also found that the optical emission of 94.6% of solar flares lasts no more than one hour. “Super-long” flares ($t > 60$ minutes) exist within 2–3 hours, whereas the lifetime of the most powerful flares is no more than 8 hours. Low-power flares, in contrast to 6–10 minutes according to Smit, Smit (1966), last on average 20 minutes. At the same time, the spread of the distribution of the duration of small flares is quite wide and amounts to ~6 hours, which is comparable to large flares.

A high correlation dependence between the duration and the rise time to maximum brightness was first found for low-power flares (Borovik, Zhdanov, 2019). On the distribution of the relative rise duration, a sequence of maxima was found,

the most significant of which are 0.2, 0.25, 0.33, and 0.5 (Fig. 1). A similar structure of the T_{rel} distribution was also shown by the types of small flares D, G, and V (Fig. 2). It should be noted that such maxima are not observed on the distributions of the duration and rise time of flare brightness. This may indicate that in small-scale optical flares, energy release occurs in a discrete manner.

Data have also been obtained showing that low-power flares exhibit development scenarios similar to those of large flares: they are accompanied by activations and eruption of filaments, have an explosive phase and multiple intensity bursts. Among them, there are flares covering sunspot umbrae, two-ribbon and white-light flares.

3.1 Energy of solar flares in the optical range

The results of the statistical analysis made it possible to estimate the total energy of flares in the optical wavelength range. According to Kurochka, Rossada (1981), the total energy of flares in all lines and continua of the hydrogen series

is closely related to the radiation energy in the H α line:

$$E_t = 4.7 \times 10^{-22} \times \alpha(i) \times S(i) \times T(i) \times I_{3,2}^2(i),$$

where i is the flare class, $I(i)$ is the central intensity of H α , $S(i)$ is the typical flare area, $T(i)$ is the typical flare lifetime, $\alpha(i)$ is a coefficient that takes into account the intensity distribution in a flare. Using the data of $\alpha(i)$ and $I_{3,2}(i)$ from Kurochka,

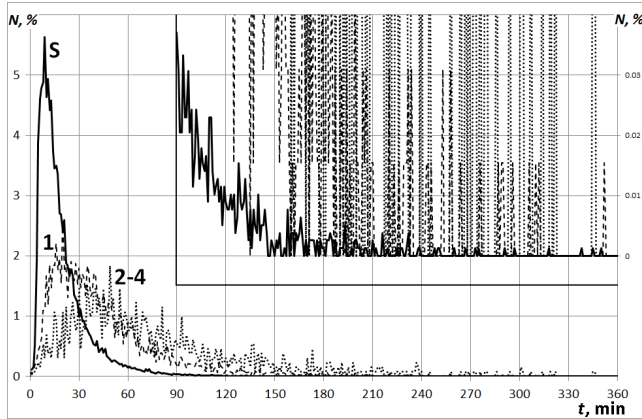


Fig. 4. Distribution of flares of area classes S, 1, and 2–4 by duration (Borovik, Zhdanov, 2017a).

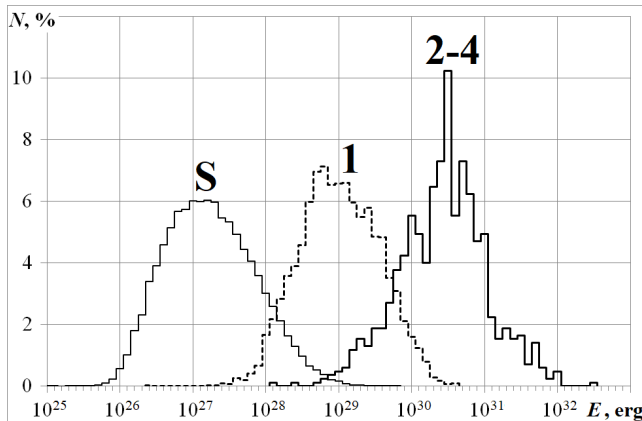


Fig. 5. Distribution of solar flares by total energy in the optical range depending on the area class (Borovik, Zhdanov, 2019).

Rossada (1981) and the distributions of flares by area $S(i)$ and duration $T(i)$ (Figs. 3 and 4), the distributions of solar flares by energies, depending on the area class and flare class, were obtained (Fig. 5). From the histograms, it follows that there is a mutual overlap in energies between the optical flares of different area classes, as a result of which up to 9.5% of low-power flares fall into the energy range of large solar flares (classes 2–4). The overlap with class 1 flares is even more significant (Borovik, Zhdanov, 2019). This provides evidence that low-power flares in the optical range can have energy compatible with the energy of large solar flares.

3.2 Relationship between optical and X-ray emission of solar flares

A flare event on the Sun encompasses practically all available ranges of electromagnetic radiation, as well as the emission of neutral particles, ejections, and large-scale shock waves. Analysis of the thermal and nonthermal emission of flares shows the complexity of the mechanisms underlying the occurring processes. It has been reliably established that there is a relation between the hard and the soft X-ray flux of a flare (Neupert, 1968). Regarding optical emission as part of the complex hydrodynamic response of the chromosphere to the impulsive heating by beams of the charged particles, there are no unambiguous conclusions yet (Fletcher et al., 2011; Somov, 1992; Bogachev et al., 2020). There are also no confident conclusions regarding the relationship between the area of optical flares and the power of X-ray emission (Altyntsev et al., 1982). Having a large volume of data, Borovik, Zhdanov (2020) showed that the low-power flares, like large solar flares, can be accompanied by proton fluxes and X-ray emission of various power, including class X. For example, in solar cycles 21–24⁷, out of 179 proton events, 6% (11) belong to low-power optical flares, 22% (40) to area class 1 flares, and 72% (128) to large flares (2–4). Out of 369 flares of X-ray class X, low-power flares account for 9%; class 1 flares, 22%; and large flares (2–4), 69%. For flares of X-ray class M (4222 flares), it is 39%, 46%, and 15%, respectively.

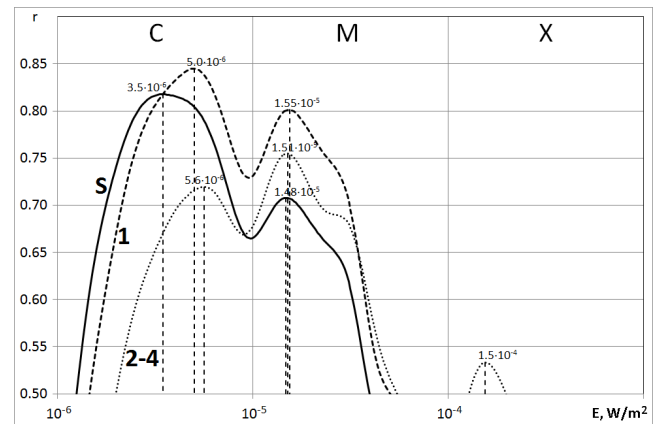


Fig. 6. Distribution of correlation coefficients between optical classes of flares and the maximum amplitude of the X-ray burst by months (09.1986–06.2017).

It was found that the correlation histograms between the area classes of optical flares and the power of X-ray emission show a significant overlap in the X-ray classes C and M (Fig. 6). The highest correlation is present between the optical flare classes S, 1 and the X-ray class C (above 0.8). For large flares (2–4), $r = 0.73$. The maximum correlation coefficients correspond to the X-ray emission power of $(3.5, 5.0, 5.6) \cdot 10^{-6}$ W/m². With an increase in the power of X-ray emission in the X-ray class M, another lower correlation maximum appears, the same for all optical flare classes

⁷ <https://umbra.nascom.nasa.gov/SEP>

and equal to the emission power of $\sim 1.5 \cdot 10^{-5} \text{ W/m}^2$. In class X, only flares 2–4 have a low correlation maximum ($r = 0.53, E = 1.5 \cdot 10^{-4} \text{ W/m}^2$).

The obtained results indicate that flares of all optical classes, including low-power flares, can be accompanied by C and M class X-ray emission with almost equal probability, and in rare cases, by powerful X-class emission.

4 Centers of flare activity of low-power flares

One of the identified characteristic features of low-power solar flares is the centers of flare activity (CFA), which are dense clusters of small flares (Fig. 7). Their contribution to the overall level of flare activity at all stages of the development of sunspot groups is decisive. As a rule, CFA have a core (sometimes two) where the density of flares is maximum. From the core to the periphery, the number of flares decreases. 93.3% of CFA are observed during one passage of an AR across the solar disk, 6.7% in two or more consecutive solar rotations, and individual centers can exist for up to four rotations. There is a high correlation of CFA with Wolf numbers ($r = 0.8$). During the passage of an AR across the solar disk, the flare activity of the CFA can last for 1.6–9 days, in some cases up to 11 days. In the region of flare activity centers, the systems of arch filaments and surges are observed, and disturbances and disappearances of filaments occur. During the intensive growth of the magnetic flux and the emergence of new magnetic fields, the frequency of flares in the centers of flare activity sharply increases, and series of flares occur.

It was found that powerful flares of optical classes 2–4 occur mainly in those active regions where CFA appear repeatedly, maintaining a stable position over several Carrington rotations. Large flares usually occur in the absence of small flares or against the background of their weak activity. On average, 7.8 hours before a large flare, small flares cease and after its onset do not occur earlier than 6.7 hours. In the regions where the ribbons of large flares develop, small flares

are also practically not found or their number is insignificant. As a result, the active region probably accumulates free magnetic energy for a large powerful flare.

The obtained results give grounds to consider the centers of flare activity as indicators of magnetic fluxes emerging on the Sun, which makes it possible to diagnose nonstationary processes in the solar atmosphere in a global aspect (Borovik et al., 2020).

5 Solar convection and low-power flares

There are many facts indicating the important role of solar convection in the origin of many active phenomena on the Sun. Convective cells (supergranules) were first discovered from observations of radial velocities at the photospheric level in the quiet regions of the Sun (Simon, Leighton, 1964). Supergranules have sizes from 20 to 54 thousand km (average value of 32 thousand km) and a lifetime of ~ 20 hours. In convective cells, the solar plasma moves from the center to the edge at a speed of 0.3–0.5 km/s, where it descends at a speed of 0.1 km/s.

According to observational materials of the full-disk of the Sun obtained with high spatial and temporal resolution at the chromospheric telescope, more than 130 low-power flares were studied. It was found that they commonly arise and develop at the boundaries of the cells of the chromospheric and the magnetic network (Figs. 8 and 9). Flare cells have an elongated ellipsoidal shape. Emission usually covers a part of the cell boundary, but in some cases the entire boundary “ignites”.

The size distribution of flare cells shows a significantly wider range than that of supergranules (Fig. 10). The average cell sizes (26 thousand km) are smaller than the average size of supergranules (32.5 thousand km). Along with the main maxima, there is a maximum at 10–12 thousand km, which indicates that the chromospheric network of active regions contains small-scale convective cells close in size to supergranular rosettes and mesogranules (5–10 thousand km).

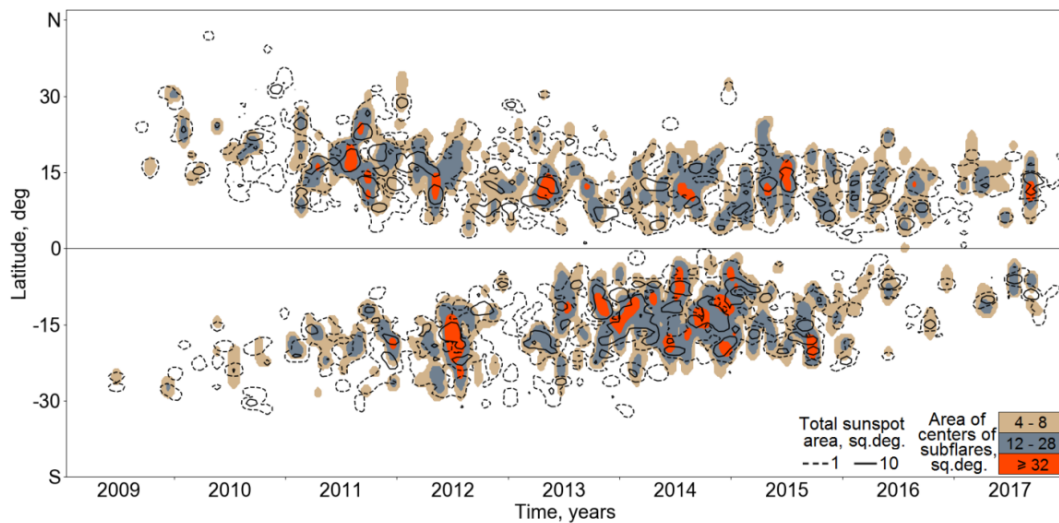


Fig. 7. Latitudinal distribution of flare activity centers in cycle 24 (Borovik et al., 2020).

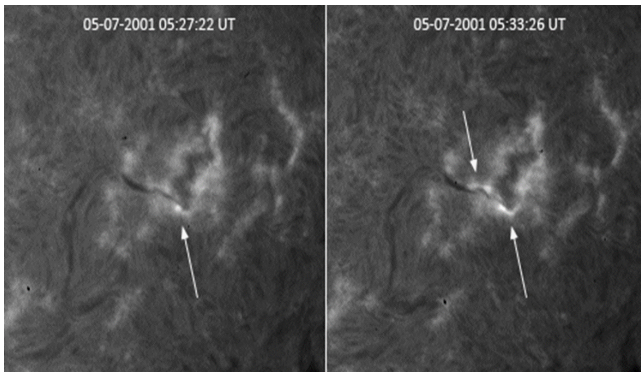


Fig. 8. Low-power flares in the $H\alpha$ line (BAO).

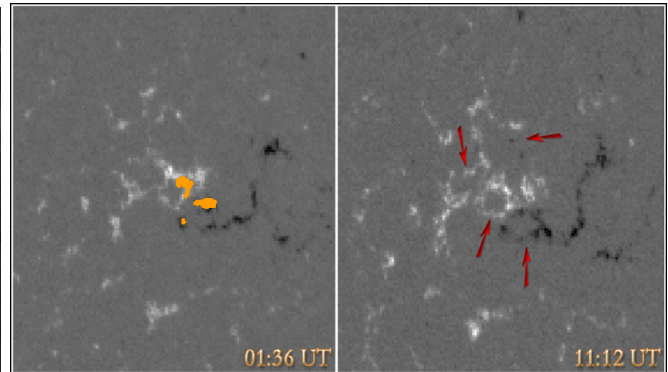


Fig. 9. Sunspotless flare on May 28, 2002. SOHO/MDI magnetograms before and after the flare. Arrows indicate evolutionary changes in the magnetic field structure of the quiet region.

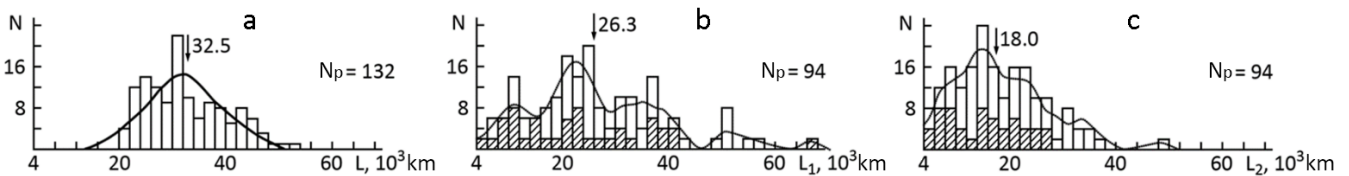


Fig. 10. Size distribution of flare cells (Borovik, 1990). Shading indicates the flares having the shape of cells. a – Leighton distribution; b – major axes of cells (L_1); c – minor axes of cells (L_2).

6 Preflare activations of chromospheric structures

The dynamic processes in the solar atmosphere preceding and accompanying flares are of great importance for the prediction and physics of solar flares. It is known that in an active region, approximately an hour before large flares, changes occur in the fine structure of the chromosphere, and activations of filaments with their complete or partial disappearance are observed. They are usually associated with local disturbances of the magnetic fields of the active region.

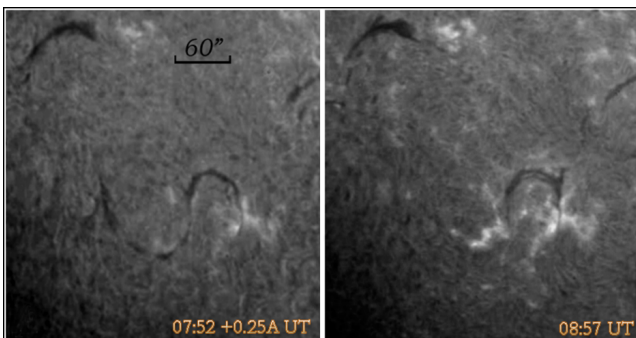


Fig. 11. Activation of a filament before the sunspotless low-power flare on 05.06.2002 (BAO).

A detailed study of preflare activations of the chromosphere before the low-power flares was performed in Borovik (1989) for 42 small flares. Only the activations associated with flare regions were considered (Figs. 11 and 12). It was found that 85% of such flares are accompanied by large-scale disturbances of the chromosphere propagating from the flare site by 90–500 thousand km, and by small-scale ones (10–60 thousand km). Large-scale activations manifest themselves 40–50 minutes before the onset of a flare; small-scale ones, within one or two nearest to the flares tiers of supergranular cells 10–20 minutes before. In 49% of cases, both types of activations were observed, in 11% only large-scale activations, and in 40% only small-scale ones. It is assumed that the cause of activations of chromospheric structures before low-power flares is large-scale disturbances of the magnetic fields of the active region.

7 Low-power flares in the developing active region SD N135 (NOAA 4520)

The connection of low-power flares with convective cells, large-scale changes in magnetic fields, and the emergence of new magnetic fluxes was confirmed in the study of the developing active region N135 (numbering of the Solar Data bulletin) within the framework of the 1984 observational program “Large-scale fields and the birth of active regions” (Borovik et al., 1986). From the first days of formation, the active region was distinguished by rapid development (Figs. 13 and 14). The intensive descending of matter occurred in it,

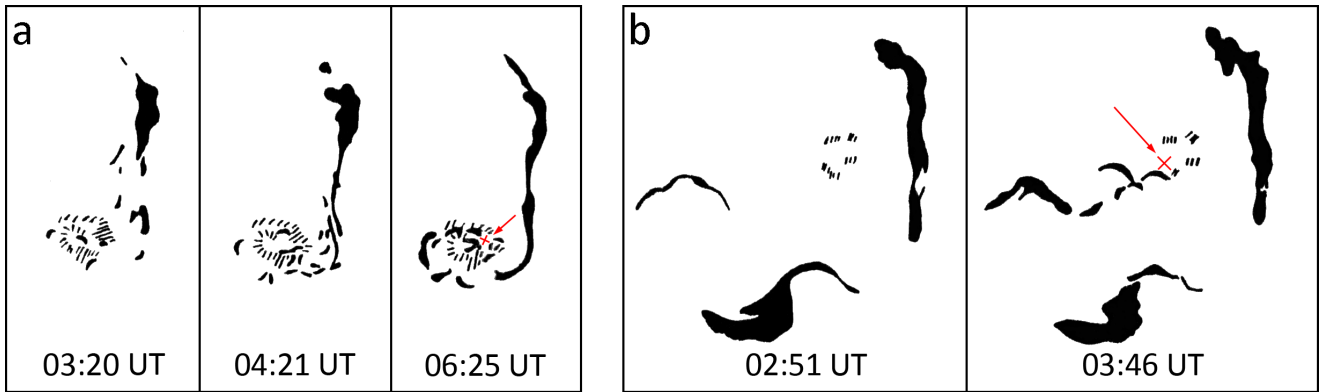


Fig. 12. Activations of filaments before low-power flares: a – flare on October 30, 1980 (S18W23); b – sunspotless flare on October 31, 1980 (N24E23). The positions of flare nodes are marked with red crosses and indicated by arrows.

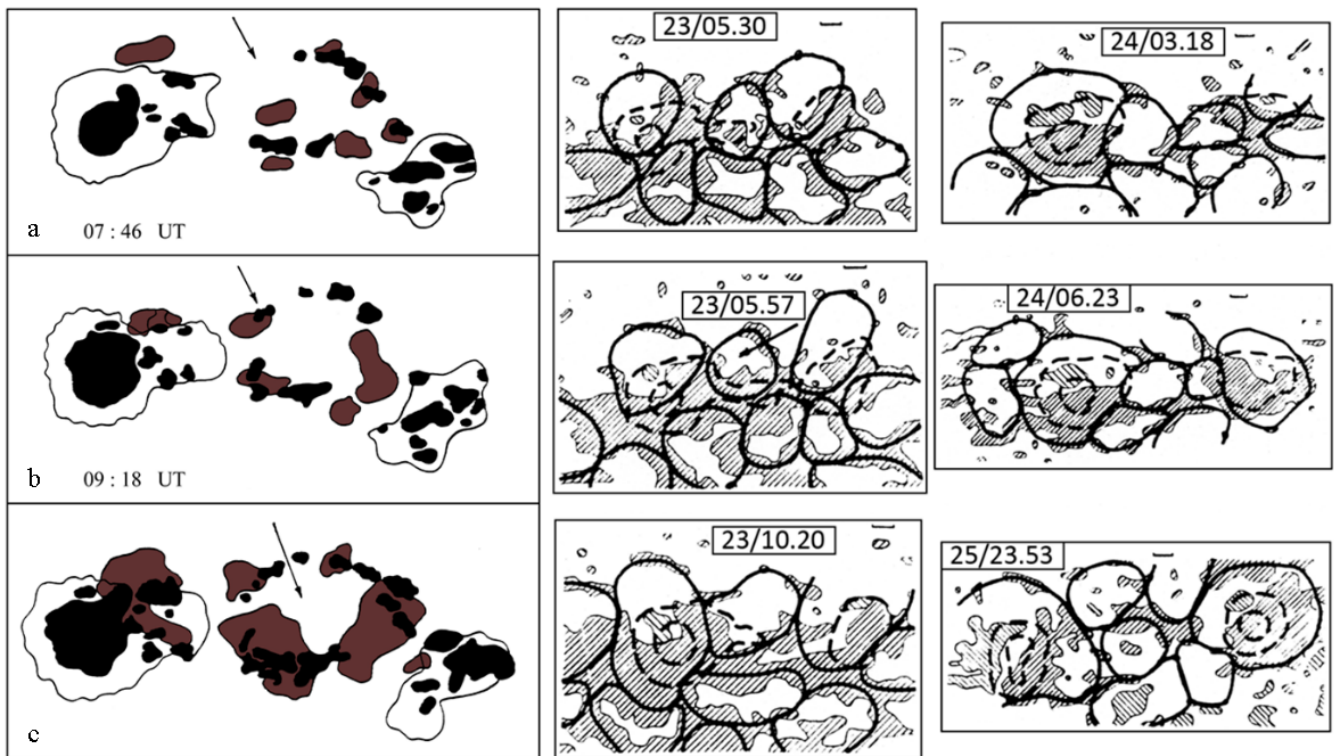


Fig. 13. Velocity field and spatial distribution of low-power flares in the active region SD N135 on June 23, 1984 (sunspots are drawn in black, flare fields in brown).

coinciding in most cases with pores and hills of the magnetic field. The dopplergrams of the Sayan Observatory of ISTP SB RAS clearly showed the ring-shaped structures of the descending flow. The size of the convective cells corresponded to the size of supergranules. A correspondence was observed between the velocity field network and the magnetic network. Changes in the structure of the cells showed that at the stage of the appearance of a sunspot and the strengthening of its magnetic flux, the sunspot was located at the boundaries of neighboring convective cells. As the AR developed, the struc-

ture of the velocity field became more complex. Changes in the integral magnetic flux and integral magnetic field strength were observed (Fig. 14b). It was during this period of growth of the magnetic field parameters that a burst of flare activity was observed (Fig. 14a), and the filament closest to the active region gradually began to increase its length (Fig. 14c,d). Small flares sequentially appeared along the boundary of the convective cell with a size of 26 thousand km (indicated by the arrow in the right panel of Fig. 13). On the photosphere, the cell was “traced” by chains of small sunspots and pores;

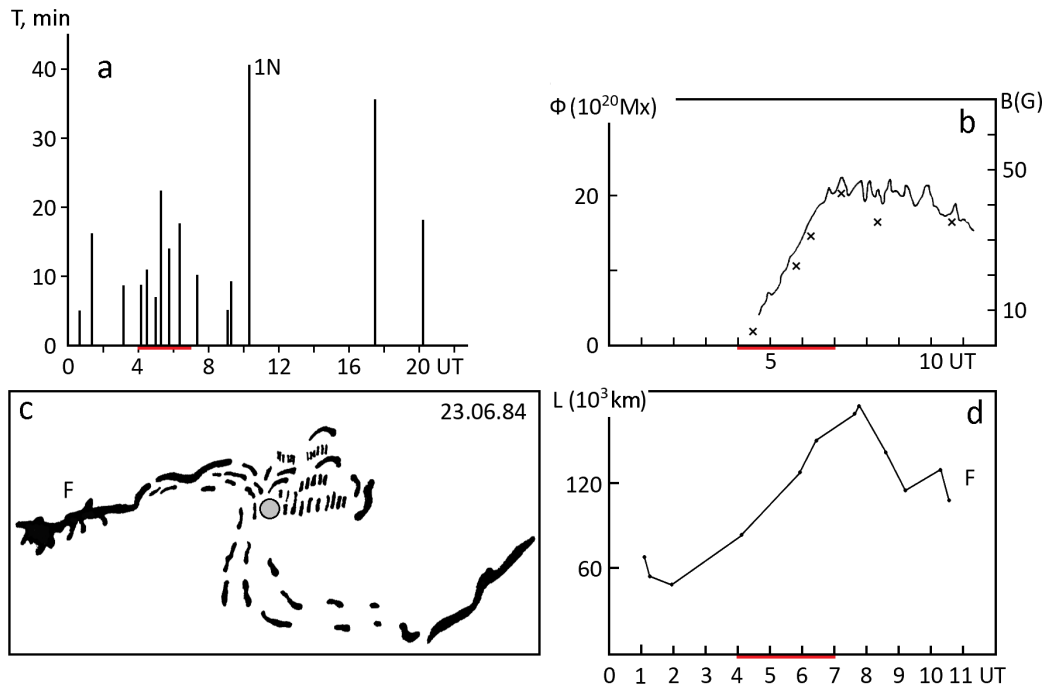


Fig. 14. Low-power flares on June 23, 1984, in the developing active region SD N135 (Borovik et al., 1986): a – development of flare activity; b – change in the integral magnetic flux (Φ) and integral magnetic field strength (B); c, d – change in the filament length F .

in the chromosphere, it coincided with a cell of the chromospheric network. Flare nodes were located near the groups of small unstable sunspots. In Figure 13a,b, arrows indicate a case when the appearance of a low-power flare coincided in place and time with the appearance of two small pores in the AR. Figure 13c shows a combined picture of the location of sunspots and low-power flares in the active region on June 23, 1984.

8 Sunspotless flares

The main difference between sunspotless flares and flares in sunspot groups is their occurrence in the undisturbed “quiet” regions of the Sun. Sunspotless flares are believed to be more prolonged, show a slow increase in brightness to the maximum and a rather extended decay. They can be quite powerful and accompanied by bursts of microwave and soft X-ray radiation (Dodson, Hedeman, 1970). During the years of solar activity minimum, the number of sunspotless flares almost doubles.

It was found (Borovik, Myachin, 2002) that sunspotless flares, like flares in sunspot groups, are preceded by a period of evolution of the magnetic fields of the “quiet” region, accompanied by the activation of filaments and a large-scale change in the fine structure of the chromosphere (Fig. 15). The highest frequency of preflare events and phenomena occurs, as in sunspot groups, in the interval of 10–60 minutes before the onset of a flare. It is worth noting that the rich fine structure of quiet regions reacts to changes in magnetic fields quite clearly (in developed active regions, it is mostly suppressed). As a result, previously unknown or extremely rare preflare disturbances of the chromosphere were discovered:

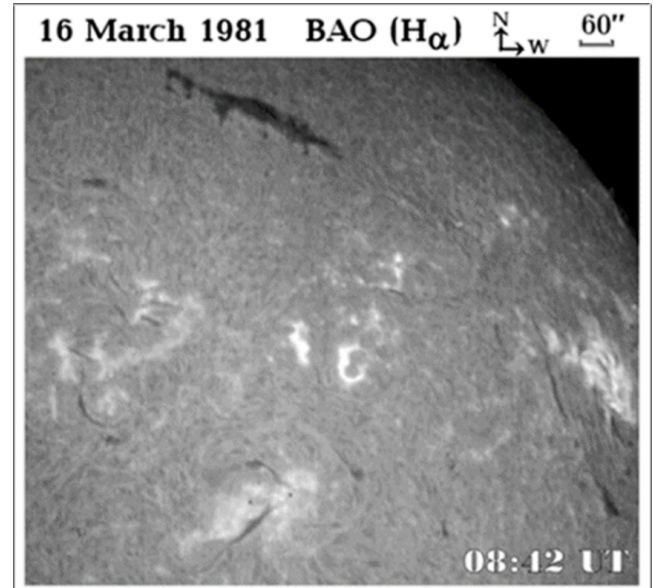


Fig. 15. Sunspotless flare on March 16, 1981, according to observations in the H_α line at the Baikal Astrophysical Observatory.

S-type vortex structures, dark cells, “ribbon channels”, preflare changes in the intensity of dark nodes in the flare region (Borovik, Myachin, 2002). The obtained results convince that the cause of such disturbances is large-scale changes in the magnetic fields of the quiet region.

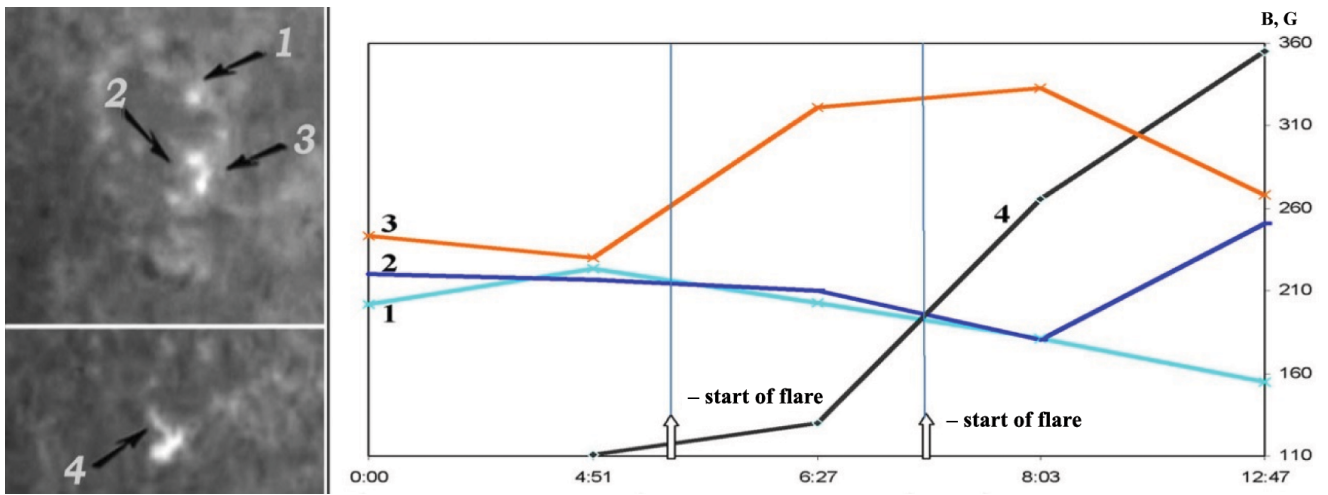


Fig. 16. Changes in the field strength in magnetic hills during the sunspotless flares on June 28, 2001 (Borovik et al., 2014).

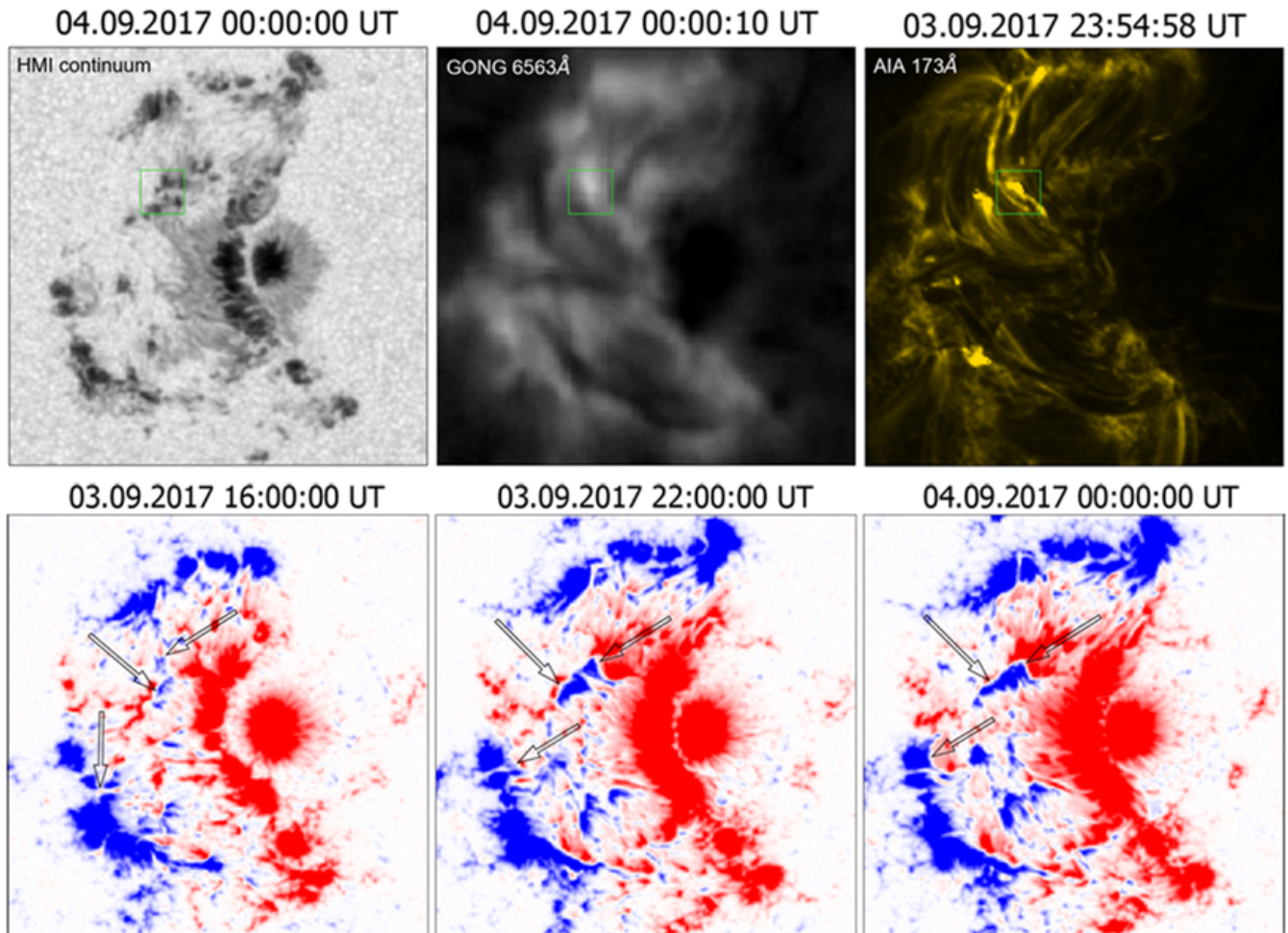


Fig. 17. Formation of local PIL in the active region NOAA 12673. In the SDO/HMI magnetograms, the fields of the northern and southern polarity are highlighted in blue and red, respectively. Arrows indicate three regions of LPIL formation.

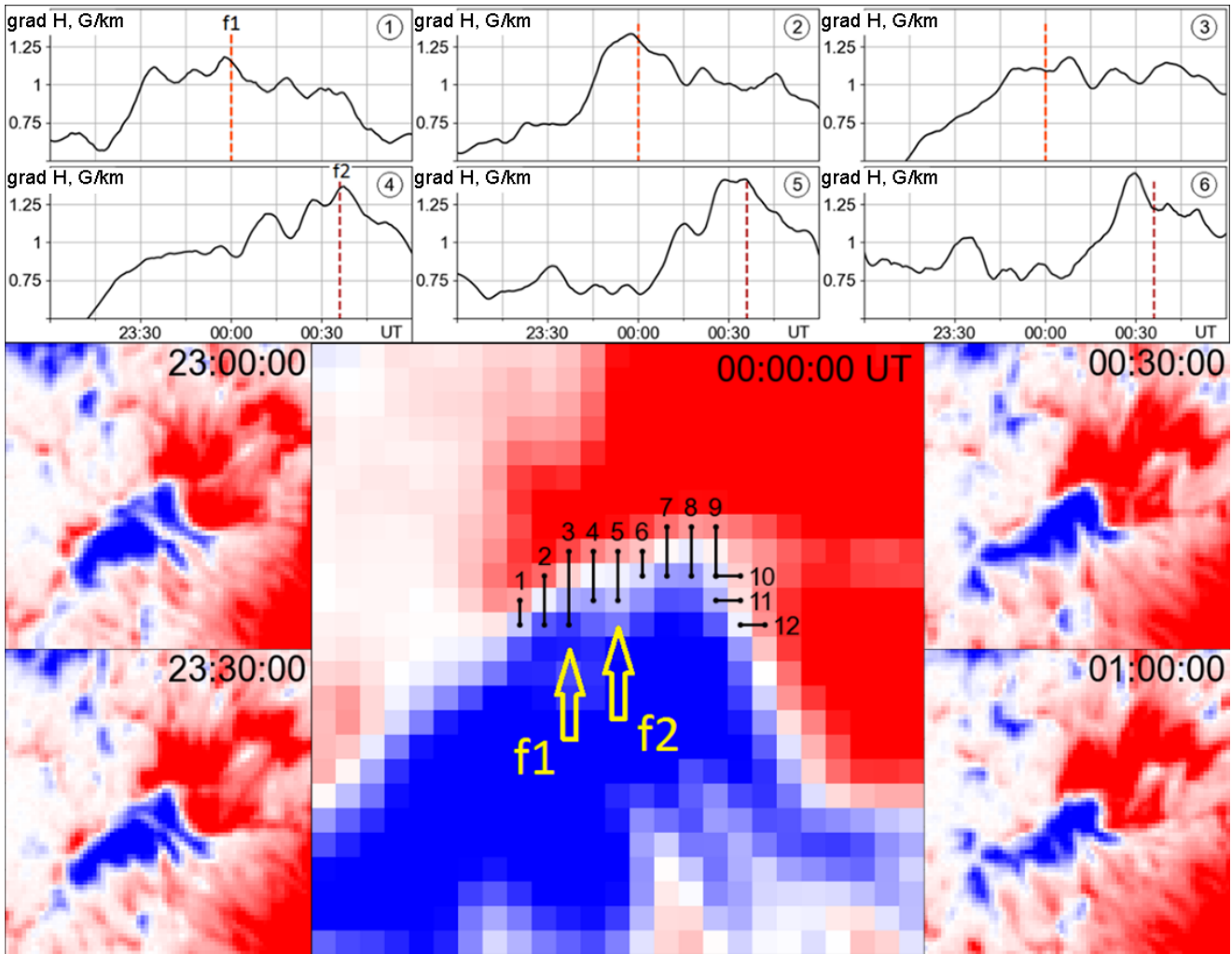


Fig. 18. Change in the gradient of the longitudinal magnetic field near the LPIL in the region of low-power flares (f1, f2). f1 is shown in Fig. 17.

As a rule, sunspotless flares occur at the boundaries of the chromospheric and magnetic networks near the hills of the enhanced magnetic field (Fig. 16) in which an increase in strength is observed during flares (in some cases, several times).

The development of flare emission, as in active regions with sunspots, occurs along the boundaries of convective cells sequentially from one magnetic hill to another. The diffuse parts of flares are usually located in the regions of weak fields and fade out first. The brightest parts of the flare, with which, as established by (Svestka et al., 1982), coronal flare loops are associated, exist for the longest time. The ribbons of sunspotless flares can occur at a considerable distance from the polarity inversion line, and the divergence of the ribbons may not be observed.

The results of Falciani, Rigutti (1972) regarding the presence of the isophote compression effect in flares were first confirmed. The study of the isophotometric structure of the sunspotless flare on March 16, 1981, shows that the nature of the change in the parameters of the intensity pulsations of flares in the $H\alpha$ line carries information about the dynam-

ics of flare processes occurring in the corona: reconnection of magnetic arcades, injection of particles into the chromosphere. The method of studying the isophotometric structures of solar flares modified by us provides additional opportunities for a comprehensive study of flare processes occurring at different levels of the solar atmosphere.

The results of the conducted research show that most of the events and phenomena accompanying flares in sunspot groups are also observed in the quiet regions of the Sun during flares. This indicates that the conditions for the occurrence of flares in the quiet regions of the Sun undisturbed by sunspots do not fundamentally differ.

9 Low-power flares and polarity inversion lines of active regions

The study of the active region NOAA 12673 confirmed that low-power flares occur during large-scale changes in the magnetic field of the active region (Figs. 17 and 18). It was found that, in contrast to large solar flares, small flares occur near

the LPIL, which are formed as a result of the emergence of new magnetic fluxes in the active region with their subsequent movement (under the action of surface flows of the solar plasma) and convergence with fluxes of opposite polarity. The occurrence of small flares is probably caused by the growth of the magnetic field gradient to values of 1.3–1.5 G/km, observed in a separate section of the LPIL in the flare region (Borovik, Zhdanov, 2022). The length of such sections is ~ 1 –1.5 arcsec. No such phenomena were observed in other sections of the LPIL.

According to modern model concepts, such processes lead to the formation of current sheets, reconnection of magnetic field lines of opposite direction, and impulsive release of free magnetic field energy in the form of a flare. Analysis of the powerful flare on September 6, 2017, of X-ray class X9.3 showed that a similar phenomenon was observed before it. In this case, the gradient of the magnetic field in a separate section of the main PIL reached a value of 3–3.5 G/km.

10 Conclusions

As a result of the conducted research, we have obtained the most complete to date and statistically reliable data on the parameters of solar flares in the H α line. For low-power flares, a high correlation was found between the duration and the rise time of brightness to the maximum. Evidence has been obtained that the energy release in low-power flares is discrete in nature.

From the point of view of development features, it has been established that low-power flares do not fundamentally differ from more powerful solar flares. Both in active and quiet regions of the chromosphere, they are accompanied by development scenarios similar to those of large powerful flares. The obtained results show that most of the preflare phenomena in the chromosphere accompanying solar flares reflect the general dynamics of the magnetic fields of active regions, as a result of which only in some cases conditions for flares arise. A feature of small flares is their close relation to hills of the enhanced magnetic field at the boundaries of the chromospheric and magnetic networks and the small-scale local short-lived polarity inversion lines of active regions. One of the possible conditions for the occurrence of low-power flares, as well as large flares, is the growth of the magnetic field gradient in the flare region to a certain critical value. According to observations, this occurs as a result of the convergence of magnetic fields of opposite direction in a separate section of the polarity inversion line, which, according to model concepts, leads to the formation of a current sheet, reconnection of magnetic field lines, and a flare.

It is assumed that the significant overlap of the distributions of low-power flares in terms of time parameters, energy, and power of X-ray emission with flares of higher area classes may be due to the energy carried by the charged particles accelerated from the coronal source into the chromosphere, and the conditions (mechanisms) of its propagation in the chromosphere.

As a result of the conducted research, a new development of the role and place of low-power solar flares in the general structure of solar activity is given. The obtained results can be used to predict solar activity, geoeffective solar events, and to

construct physical models. The work was carried out within the framework of the state assignment II.16 and supported by the RFBR grant 19-52-45002.

References

- Altyntsev A.T., Banin V.G., Kuklin G.V., Tomozov V.M., 1982. Solar flares, M.: Nauka. (In Russ.)
- Bogachev S.A. et al., 2020. Uspekhi fizicheskikh nauk, vol. 190, no. 8, pp. 838–858. (In Russ.)
- Borovik A.V., 1989. Issled. po geomagnetizmu, aeronomii i fizike Solnca, vol. 87, pp. 154–166. (In Russ.)
- Borovik A.V., 1990. Issled. po geomagnetizmu, aeronomii i fizike Solnca, vol. 91, pp. 63–73. (In Russ.)
- Borovik A.V., Myachin D.Yu., 2002. Solar Phys., vol. 205, pp. 105–116.
- Borovik A.V., Zhdanov A.A., 2017a. Solar-Terrestrial Physics, vol. 3, no. 1, pp. 40–56.
- Borovik A.V., Zhdanov A.A., 2017b. Solar-Terrestrial Physics, vol. 3, no. 4, pp. 5–16.
- Borovik A.V., Zhdanov A.A., 2018a. Solar-Terrestrial Physics, vol. 4, no. 3, pp. 3–12.
- Borovik A.V., Zhdanov A.A., 2018b. Solar-Terrestrial Physics, vol. 4, no. 2, pp. 8–16.
- Borovik A.V., Zhdanov A.A., 2019. Solar-Terrestrial Physics, vol. 5, no. 4, pp. 3–9.
- Borovik A.V., Zhdanov A.A., 2020. Solar-Terrestrial Physics, vol. 6, no. 3, pp. 16–22.
- Borovik A.V., Zhdanov A.A., 2022. Solar-Terrestrial Physics, vol. 8, no. 1, pp. 19–23.
- Borovik A.B., Grigoryev V.M., Kargapolova N.N., et al., 1986. Contributions of the astronomical observatory Skalnaté Pleso, vol. 15, pp. 211–242. (In Russ.)
- Borovik A.V., Myachin D.Yu., Tomozov V.M., 2014. Izvestiya IGU. Ser. Nauki o Zemle, vol. 7, no. 1, pp. 23–45. (In Russ.)
- Borovik A.V., Mordvinov A.V., Golubeva E.M., and Zhdanov A.A., 2020. Astron. Rep., vol. 64, no. 6, pp. 540–546.
- Dodson H.W., Hedeman E.R., 1970. Solar Phys., vol. 13, no. 2, pp. 401–419.
- Falciani R., Rigutti M., 1972. Solar Phys., vol. 26, pp. 114–116.
- Fletcher L. et al., 2011. Space Sci. Rev., vol. 159, no. 1–4, pp. 19–106.
- Heyvaerts J., Priest E.R., Rust D.M., 1977. Solar Phys., vol. 53, no. 1, pp. 255–258.
- Howard R., Harvey J.W., 1964. Astrophys. J., vol. 139, no. 5, pp. 1328–1335.
- Kurochka L.N., Rossada V.M., 1981. Solnechnye dannye, no. 7, pp. 95–100. (In Russ.)
- Neupert W.M., 1968. Astrophys. J., vol. 153, pp. L59–L64.
- Prist E., 1985. Solar magnetic hydrodynamics, M.: Mir. (In Russ.)
- Severnyi A.B., Shaposhnikova E.F., 1961. Izv. Krymsk. Astrofiz. Observ., vol. 24, pp. 235–257. (In Russ.)
- Simon G.W., Leighton R.B., 1964. Astrophys. J., vol. 140, pp. 1120–1147.
- Smit G., Smit E., 1966. Solar flares, M.: Mir. (In Russ.)

Somov B.V., 1992. Physical processes in solar flares, Dordrecht, Boston: Kluwer Academic Publishers.

Svestka Z., 1975. In Shea M.A., Smart D.F. (Eds.), Results obtained during the campaign for integrated observations of solar flares (CINOF). Special reports, AFCRL-TR-

75-0437. Air Force Cambridge Research Labs., no. 193, pp. 9–23.

Svestka Z. et al., 1982. Solar Phys., vol. 75, no. 1–2, pp. 305–329.